Effect of pH on the Iso-1-cytochrome *c* Denatured State: Changing Constraints Due to Heme Ligation[†]

Christopher R. Smith, Eydiejo Wandschneider, and Bruce E. Bowler*

Department of Chemistry and Biochemistry, University of Denver, 2190 East Iliff Avenue, Denver, Colorado 80208

Received September 9, 2002; Revised Manuscript Received December 27, 2002

ABSTRACT: The effect of pH on the denatured state (3 M guanidine hydrochloride) was evaluated with fluorescence spectroscopy for four variants of iso-1-cytochrome *c*, AcTM (no surface histidines), AcH26 (surface histidine at position 26), AcH54 (surface histidine at position 54), and AcH54I52 (stabilizing I52 mutation added to AcH54). Changes in the compactness and the heme ligation of the denatured state, as a function of pH, were monitored through changes in Trp 59−heme fluorescence quenching. With the AcTM and AcH26 variants, no change in the fluorescence intensity occurs from pH 4 to 10. However, for the AcH54 and AcH54I52 variants the fluorescence intensity drops significantly between pH 4 and 6, consistent with His 54 binding to the heme of cytochrome *c*. Between pH 8 and 10 fluorescence intensity increases again, indicating that the His 54 is displaced from the heme. The data are consistent with lysines 4 and 5 being the primary heme ligands at alkaline pH, under denaturing conditions. This conclusion was confirmed by site-directed mutagenesis. Thermodynamic analysis indicates that heme−ligand affinity in the denatured state is controlled primarily by sequence position (loop size) and that when histidines are present they inhibit lysine ligation until approximately pH 8.5−9.0 as compared to pH 7.5 with the AcTM variant. Thus, at physiological pH, histidine ligands provide the primary constraint on the denatured state of cytochrome *c*. The heme−Trp 59 distance in the denatured state of iso-1-cytochrome *c*, derived from analysis by Förster energy transfer theory, is ∼26 Å at pH 4 and 10, much shorter than the random coil prediction of 56 Å. Surprisingly, the heme−Trp 59 distance in the His 54 bound conformation only drops to ∼21 Å, consistent with an extended conformation for the short polypeptide segment separating heme and Trp 59.

The process of folding a protein from a structurally disordered state to a well-defined three-dimensional structure capable of biological activity has generated strong interest in recent years (*1*−*4*). Considerable effort has been directed at how this complex conformational search might be limited (*5*, *6*). In particular, researchers have focused on folding intermediates (*1*) or pre-organization in the denatured states of proteins (*7*, *8*) as potential means for limiting this search. With regard to the latter possibility, studies on the hydrodynamic properties of proteins in 6 M guanidine hydrochloride (gdnHCl)[1] indicated that proteins behaved as random coils under these conditions (*9*). More recently, however, NMR studies have demonstrated that residual structure in proteins is not uncommon (*10*, *11*) and in fact can be substantial for proteins that unfold in the absence of denaturants (*12*−*14*). In the case of staphylococcal nuclease, the overall topology of the native state appears to be maintained even under strongly denaturing conditions (*15*, *16*). Thermodynamic studies, in this laboratory, on loop formation under denaturing conditions also have indicated significant deviations from random coil behavior for iso-1-cytochrome *c* in 3 M gdnHCl (*17*−*20*). Thus, there is strong evidence that structural constraints in denatured proteins may provide one avenue to limit the conformational search required to fold a protein.

When cytochrome *c* is denatured either with gdnHCl or urea, the Met80 heme ligand (in the sixth coordination site of the heme) is replaced by a histidine ligand (*21*, *22*). For horse cytochrome *c*, the histidines at positions 26 and 33 compete for the sixth iron coordination site in the denatured state near neutral pH (*23*), although His 33 appears to be the predominant ligand (*24*). For the yeast iso-1-cytochrome *c*, histidines 26, 33, and 39 all compete for heme binding in the denatured state, with similar affinity (*18*, *19*). Studies on the folding kinetics of horse and yeast cytochromes *c* at low pH or with histidines removed by mutagenesis methods have shown that histidine misligation slows the folding of cytochrome *c* (*24*−*27*). Thus, constraining the denatured state in a non-native manner inhibits the folding of the protein. In the case of iso-1-cytochrome *c*, ligation of the N-terminal amino group to the heme also slows folding (*27*).

[†] This work was supported by NIH Grant GM57635 (B.E.B.) and a Partners in Scholarship Grant from the University of Denver (C.R.S.). The NSF Grant 9977691 is acknowledged for support of the Beckman CEQ2000 DNA analysis system.

* To whom correspondence should be addressed. Phone: (303) 871-2985. Fax: (303) 871-2254. E-mail: bbowler@du.edu.

[1] Abbreviations: NATA, *N*-acetyltryptophanamide; gdnHCl, guanidine hydrochloride; AcTM, variant of iso-1-cytochrome *c* with no surface histidines and with N-terminal acetylation; AcHX, AcTM variant of iso-1-cytochrome *c* with a single histidine added at position number X; AcQX, AcTM variant of iso-1-cytochrome *c* with a lysine converted to glutamine at position number X. Amino acid mutations are indicated using single letter amino acid codes and the sequence position as follows: H26N, for example, means that the histidine at position 26 is replaced with asparagine.

10.1021/bi026827i CCC: $25.00
Published on Web 01/30/2003

Under denaturing conditions (3 M gdnHCl), a variant of iso-1-cytochrome *c* that is N-terminally acetylated in vivo and has no surface histidines, AcTM (contains mutations T(-5)S, K(-2)L, H26N, H33N, and H39Q, see ref *19*), still shows a high spin to low spin transition for the heme with an apparent pK_a, pK_a(obs), of ~7.5 in 3 M gdnHCl. This observation indicates that the sixth coordination site of cytochrome *c* is filled by another strong field ligand, presumably lysine, under denaturing conditions near physiological pH. Other recent work has also implicated lysine as a heme ligand in non-native states of the protein (*28*). Since topological constraints on the denatured state of cytochrome *c*, because of other heme ligands, can occur near physiological pH, it is of interest to determine the identity of these ligands, the topological constraint they impose, and how well they compete with histidine for heme ligation. Different constraints imposed by different ligands are expected to affect the folding mechanism of this protein.

Since the visible absorption properties of the low spin heme are not strongly sensitive to the nature of the strong field ligand, it has been difficult to determine over what pH range histidine is the predominant ligand under denaturing conditions. Another possible means of obtaining this information is through measuring changes in the fluorescence of Trp 59 as a function of pH, under denaturing conditions. The quenching of the fluorescence of the single tryptophan residue at position 59 by the heme moiety provides information on the dimension of the denatured state (*29*). In the native form of cytochrome *c*, there is virtually no fluorescence because Trp 59 is in direct contact with the heme (*30*), leading to efficient energy transfer from the Trp 59 donor to the heme acceptor and causing complete quenching of tryptophan fluorescence. As the protein unfolds, the distance between the Trp 59 and the heme increases causing the fluorescence to increase (*29*). It is well-documented that Trp 59 quenching, and thus the Trp 59−heme distance, is sensitive to denaturant concentration (*29*) and pH (*31*). Therefore, we have monitored Trp 59 fluorescence as a function of pH under denaturing conditions (3 M gdnHCl) with several iso-1-cytochrome *c* variants to explore heme ligation in denatured cytochrome *c*.

In addition to providing information about changes in heme ligation, the dimension of the denatured state of cytochrome *c* as a function of pH can be assessed using this Trp 59−heme spectroscopic ruler (*32*). The R_o of the Trp−heme donor−acceptor pair is ~30 Å (*26*, *33*), and it has been well-demonstrated in a number of studies that this R_o is well-suited to monitoring changes in the dimensions of denatured cytochrome *c* (*26*, *29*, *31*, *34*). There is great interest in the compactness of denatured states (*7*) and to what extent protein denatured states approximate a random coil. Thus, we evaluate our fluorescence data with respect to an unquenched donor, *N*-acetyltryptophanamide (NATA), and compare the results to the expected dimension of a random coil polypeptide (*9*, *35*, *36*).

Finally, the fluorescence studies on gdnHCl denatured iso-1-cytochrome *c* variants narrowed the possibilities for the predominant heme ligands causing the denatured state pK_a-(obs) of ~7.5 (*19*) for the AcTM variant of iso-1-cytochrome *c*. Several single histidine variants as well as lysine knockout variants were prepared to confirm the identity of the high pH denatured state ligands for iso-1-cytochrome *c*. Thermodynamic analysis of the data from these variants, in combination with the fluorescence results, allows the competition between histidine and other ligands to be assessed. The analysis also demonstrates that the sequence position of the heme ligand (loop size formed when bound to the heme) is the primary determinant of its affinity for the heme under denaturing conditions.

MATERIALS AND METHODS

Preparation of Iso-1-cytochrome c Variants. AcTM, AcH26, AcH27, AcH54, and AcH54I52 (in the nomenclature AcHX, Ac indicates N-terminal acetylation in vivo, H indicates the presence of a single histidine besides His 18, and X gives the sequence position of the histidine) were isolated and purified as described previously (*19*, *37*). The AcH54I52 variant (*37*) contains the stabilizing mutation Asn 52 → Ile (*38*).

New variants used in this work were prepared using the unique restriction site elimination site-directed mutagenesis method (*39*), as previously described (*19*, *20*). In all cases, pRS/C7.8 singled-stranded DNA (*19*, *20*) containing the sequence for the AcTM variant of iso-1-cytochrome *c* was used as the template for site-directed mutagenesis. The mutated DNA for the AcH22 variant and the lysine → glutamine variants AcQ11, AcQ22, AcQ27, AcQ4Q5, and AcQ54Q55 (in the nomenclature AcQX, Ac indicates N-terminal acetylation in vivo, Q indicates a glutamine replacing a lysine, and X gives the sequence position number of the glutamine) were prepared in this manner. In all cases, the selection oligonucleotide, *Sac*I+II− (*19*, *20*) was used in combination with an appropriate mutagenic oligonucleotide to generate the desired mutation. The presence of the desired mutation was confirmed by DNA sequencing using a Beckman CEQ2000 automated DNA sequencer.

For each variant, mutant double-stranded pRS/C7.8 DNA was transformed into *Saccharomyces cerevisiae* GM-3C-2 cells (cytochrome *c* deficient), and the mutant cytochrome *c* was tested for functionality, as previously described (*40*). The transformed cells were then subjected to a curing procedure to ensure that the cytochrome *c* phenotype was plasmid-based, as previously described (*40*). The pRS/C7.8 DNA was then recaptured from GM-3C-2 cells and resequenced with the Beckman CEQ2000 to confirm that no mutations had occurred under the selective pressure of the expression system (*40*). Variant proteins were then isolated and purified, as described above.

Denatured State Fluorescence Spectroscopy Experiments. To oxidize the desired cytochrome *c* variant, ~5 mg of potassium ferricyanide was added to ~200 μL of protein that was at a concentration of ~7 mg/mL. The potassium ferricyanide was allowed to oxidize the cytochrome *c* for 45−60 min. Then, the protein was run down a G-25 column equilibrated to 3X buffer (15 mM Tris and 45 mM NaCl, pH 9.2) to separate the oxidized cytochrome *c* from the potassium ferricyanide. The concentration and degree of oxidation was then determined spectrophotometrically, as described previously (*40*). A 3X protein (9 μM) solution in 3X buffer was then prepared by dilution with 3X buffer. The actual concentration of the 6 M gdnHCl stock was then found using refractive index measurements (*41*) and was always within 1% of 6 M.

The experiment consisted of using two fluorescence cuvettes with 2 mL of the appropriate solution in each. The protein cuvette consisted of 1 mL of 6 M gdnHCl, 667 μL of 3X protein solution in 3X buffer, and 333 μL of doubly deionized water, ddH_2O (Barnstead Nanopure Infinity Ultrapure Water System). The blank cuvette consisted of 1 mL of 6 M gdnHCl, 667 μL of 3X buffer, and 333 μL of ddH_2O and served the purpose of a nonfluorescent blank. Thus, both cuvettes were 3 M in gdnHCl and 1X in buffer. The protein cuvette had a working concentration of 3 μM protein. The cuvettes were mixed with stir bars for a few minutes, and then the pH of the cytochrome *c* containing cuvette was measured. The starting pH for the protein cuvette was then adjusted to the range of 3−4. When lowering the pH of the protein containing cuvette, a 3:2:1 ratio of the following three stock solutions was used, respectively, 6 M gdnHCl, 3X protein solution in 3X buffer, and aqueous HCl of appropriate concentration. Once the protein cuvette had been lowered to the desired starting pH, exactly the same total volume of each stock solution was added to the blank cuvette, except that 3X buffer was used in lieu of the 3X protein in 3X buffer stock.

The fluorescence of the samples was then measured using a Spex Fluorolog 2 spectrofluorimeter. The samples were excited at 287 nm, and the fluorescence intensity was measured at 350 nm. Both excitation monochromator slit widths were set to 4 mm and both emission monochromator slit widths were set to 2 mm. To adjust the pH upward, 1 μL of an appropriate concentration of sodium hydroxide (NaOH) solution was added to each of the cuvettes, along with 2 μL of the of 3X protein in 3X buffer or the 3X buffer stock, as appropriate, and 3 μL of the 6 M gdnHCl stock. Thus, the concentrations of protein, gdnHCl, and buffer were maintained at constant values throughout the experiment; only the pH varied. The pH of the protein cuvette was measured, followed by fluorescence measurements for each cuvette. This process was continued until the pH was between 10 and 11. Measurements of the final pH of the blank cuvette showed that it was within 0.1 pH units of the protein cuvette used to track pH during the experiment.

For experiments on the AcH54I52 variant, a third cuvette containing *N*-acetyltryptophanamide, NATA (Bachem Biosciences, Inc.), at a concentration of 3 μM, was also measured concurrently with protein and blank cuvettes. The NATA was dissolved in 6 M gdnHCl. The concentration of this stock solution was evaluated spectrophotometrically ($\epsilon_{280} = 5690$ M^{-1} cm^{-1} in 6 M gdnHCl, see ref *42*). A 6 M gdnHCl stock with 6 μM NATA was prepared. The first sample was prepared using 1.0 mL of this stock, 667 μL of 3X buffer, and 333 μL of ddH_2O. Thus, this sample was 3 M in gdnHCl, 1X in buffer, and 3 μM in NATA. The pH of this sample was adjusted as described above using 3 μL of the 6 M gdnHCl, 6 μM NATA stock, 2 μL of the 3X buffer stock, and 1 μL of aqueous HCl or NaOH, as appropriate.

Denatured State pH Titrations Monitored by UV−Vis. All UV−vis monitored denatured state pH titrations were carried out, as described previously (*17*−*20*, *27*), in 3 M gdnHCl, in the presence of 5 mM Na_2HPO_4 and 15 mM NaCl. The protein was oxidized prior to each experiment, as described above. The temperature of the titration solutions was 22 ± 1 °C. Absorbance at 398 nm was plotted against pH and fit to the Henderson−Hasselbalch equation using SigmaPlot (v. 7):

$$A_{398} = \frac{(A_{398,LS} + A_{398,HS} \times 10^{n(pK_a(obs)-pH)})}{(1 + 10^{n(pK_a(obs)-pH)})} \quad (1)$$

In eq 1, pK_a(obs) is the apparent pK_a for ligand−heme binding, *n* is the number of protons involved in the process, A_{398} is the absorbance at 398 nm at a given pH, $A_{398,LS}$ is the absorbance at 398 nm of the low spin form of the heme (histidine or other strong field ligand bound in the sixth coordination site), and $A_{398,HS}$ is the absorbance at 398 nm of the high spin form of the heme (H_2O bound in the sixth coordination site). At protein concentrations >7.5 μM, the change in spin state was monitored at 380 nm (15 μM) or 620 nm (30 and 60 μM). The values reported are the average of three separate experiments at 3 μM protein concentration and two separate experiments at other protein concentrations. The error given is the larger of the standard deviation of the separate experiments or the error in the parameter from the nonlinear least-squares fit of the data obtained from the output of Sigmaplot (v. 7).

To assess the dependence of pK_a(obs) on protein concentration, the K_a(obs) data were fit to eq 2 (*20*)

$$K_a(obs) = K_{intra} + (K_{inter}/2)[Cyt\ c]_{total} \quad (2)$$

where K_{intra} is the equilibrium constant for intramolecular histidine−heme loop formation, and K_{inter} is the equilibrium constant for intermolecular histidine−heme binding.

Stability Measurements. GdnHCl denaturation monitored by circular dichroism was carried out, as described previously (*43*). All measurements were made at 25 °C in the presence of 20 mM Tris, pH 7.0, and 40 mM NaCl as buffer. The ellipticity as function of [gdnHCl] was fit to a two-state unfolding model by nonlinear least-squares methods, assuming a linear free energy relationship for the dependence of unfolding free energy, ΔG_u, on [gdnHCl] (*18*, *44*). Values for the stability in water, $\Delta G_u(H_2O)$, and the denaturant dependence of ΔG_u (*m*-value) were obtained from the fits to the data. The errors reported are the standard deviation of three separate experiments.

RESULTS

Studies on the alkaline conformational transition of cytochrome *c* show that lysine has a strong affinity for heme (*45*). Recent work on NMR-monitored unfolding of horse cytochrome *c* also implicates lysine as a heme ligand in nonnative states of the protein (*28*). There are 15 lysines in wild-type iso-1-cytochrome *c*, and we have previously postulated that one or several of these lysines may act as heme ligands under denaturing conditions above neutral pH (*27*). Work in this laboratory shows that the 37 residue loop formed by His 54 binding to the heme in the denatured state of iso-1-cytochrome *c* is unusually favorable (pK_a(obs) = 4.81 ± 0.06), making lysines 54 and 55 possible candidates for the predominate nonhistidine heme ligand in the denatured state of the AcTM variant, near pH 7.5. Similarly, we have shown (*20*) that histidines at positions 4 and −2 have very high affinity for heme in the denatured state (pK_a(obs) ∼4.2). Thus, lysines at positions 4 and 5 (to produce in vivo acetylated iso-1-cytochrome *c* the AcTM variant has had

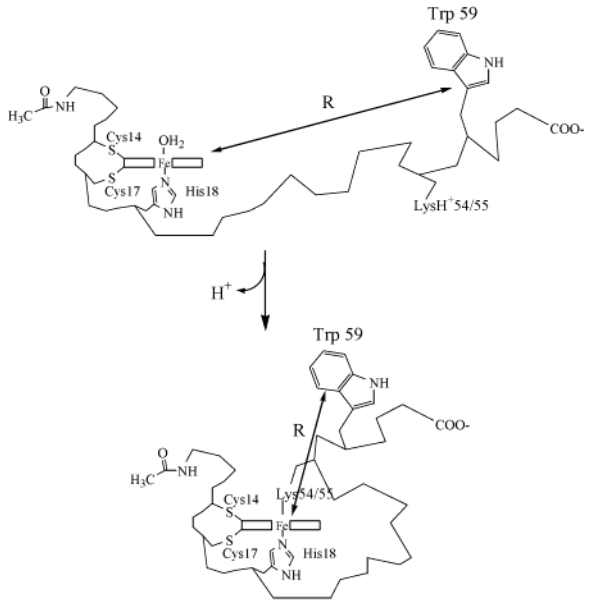

FIGURE 1: Schematic representation of the affect of binding Lys 54/55 to the heme of denatured AcTM on the Trp 59−heme distance. The double-headed arrows show the Trp 59−heme distance, *R*, for the low pH water bound state of the heme and for the high pH Lys 54/55 bound state of the heme. As shown, a single proton is released when an ionizable ligand (or ligands) binds to the iron atom of the heme. Thus, the equilibrium should be a one proton process.

Lys(-2) converted to leucine) are also strong candidates for the predominate heme ligands causing the spin state transition in the denatured state of the AcTM variant of iso-1-cytochrome *c* (pK_a(obs) ~7.5). To narrow the spectrum of possible denatured state lysine ligands and to provide direct thermodynamic assessment of the competition between lysine and histidine ligands under denaturing conditions, we first carry out studies on the pH dependence of the fluorescence intensity of the Trp 59 of iso-1-cytochrome *c* under denaturing conditions.

Fluorescence of AcTM, AcH26, and AcH54 as a Function of pH. Three proteins were chosen for pH dependent studies of Trp 59 fluorescence in the denatured state, AcTM, AcH26, and AcH54. Binding of Lys 54/55 to the heme at alkaline pH is expected to lead to significant quenching of Trp 59 fluorescence for the AcTM (no histidines bound at lower pH, see Figure 1) and AcH26 (His 26 bound at lower pH) variants as the Trp 59 is brought closer to the heme. For AcH54, no significant change in fluorescence intensity is expected at alkaline pH if Lys 55 replaces His 54. On the other hand, if lysines 4 and 5 are involved in heme binding above pH ~7.5 under denaturing conditions, little change in the fluorescence of the AcTM and AcH26 variants would be expected as a function of pH. For gdnHCl denatured AcH54, the fluorescence of Trp 59 would increase at higher pH if Lys 4/5 replaces His 54.

In Figure 2, the fluorescence intensity of Trp 59 versus pH in 3 M gdnHCl for AcTM (Figure 2A), AcH26 (Figure 2B), and AcH54 (Figure 2C) is shown. For both AcTM and AcH26, the Trp 59 fluorescence intensity does not change significantly with pH over a broad pH range. Obvious changes in the Trp 59 fluorescence intensity of AcH54 occur over the same pH range. At low pH, the fluorescence intensity of AcH54 is high, but as the pH is raised, the

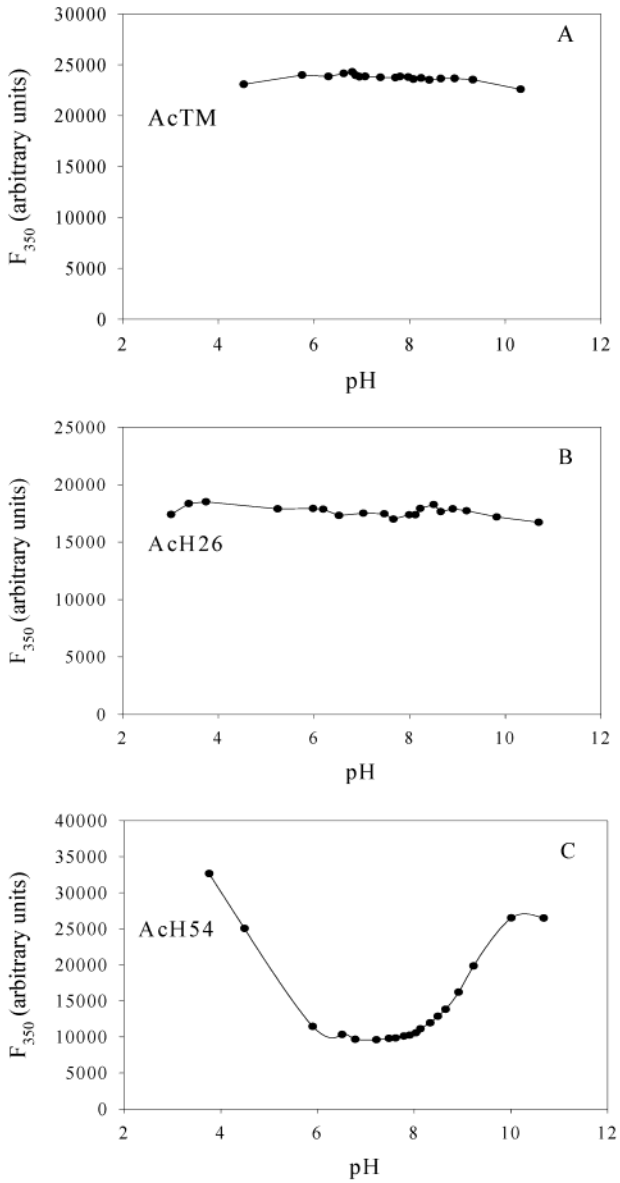

FIGURE 2: pH dependence of Trp 59 fluorescence intensity, F_{350}, for the (A) AcTM, (B) AcH26, and (C) AcH54 variants under denaturing conditions (3 M gdnHCl). The protein concentration is 3 μM. The background fluorescence of a blank sample monitored concurrently with the protein sample has been subtracted from the fluorescence of the protein sample at each pH value. Data were acquired at room temperature, 22 ± 1 °C. Excitation was at 287 nm, and emission was monitored at 350 nm. The solid curves simply connect the data points.

fluorescence intensity drops and levels out in the range of pH 6−8. Above pH 8, the fluorescence intensity rises again. The higher fluorescence intensity of AcH54 at low pH is consistent with water bound to the heme (Figure 1) and with His 18 as the last covalent contact with the heme relative to Trp 59. In the pH range 6−8, the decreased fluorescence intensity is consistent with His 54 binding to the heme and drawing Trp 59 close to the heme. Above pH 8, His 54 is clearly lost, and the increase in fluorescence intensity is inconsistent with Lys 55 acting as the predominate ligand at higher pH but consistent with Lys 4/5 acting as the ligands. The observation that the increase in fluorescence intensity occurs at higher pH than the pK_a(obs) for the AcTM variant (~7.5) indicates that His 54 binding provides significant competition for binding of the lysine ligands.

The behavior of AcTM is similarly inconsistent with Lys 54/55 as the predominate heme ligands at higher pH since no decrease in Trp 59 fluorescence intensity is observed near pH 7.5 relative to the water bound heme at low pH. From previous work, it is known that His 26 binds to the heme with a pK_a(obs) ~5.3 (*19*). Our data indicate that Trp 59 fluorescence intensity data cannot distinguish between the low pH water bound and the His 26 bound states of the heme. As with AcTM, the data provide no evidence for Lys 54/55 binding at higher pH. However, because of the insensitivity of the Trp 59 fluorescence to His 26 binding, the fluorescence data cannot rule out other lysines near the heme (lysines 11, 22, and 27) as possible heme ligands above pH ~7.5.

Quantitative Assessment of Trp 59−Heme Distance as a Function of pH. The qualitative work on the AcTM, AcH26, and AcH54 proteins indicates that AcH54 is the most interesting protein with which to pursue quantitative distance measurements using the Förster method. For convenience, we have used the AcH54I52 variant, which has the stabilizing N52I mutation, providing for greater isolated yields of protein. The pK_a(obs) for the high spin−low spin transition monitored at the heme Soret band for AcH54I52 is within error identical to that observed for the AcH54 protein (pK_a(obs) = 4.89 ± 0.03 for AcH54I52, see ref *37*; pK_a(obs) = 4.81 ± 0.06 for AcH54, see ref *19*). Thus, introduction of Ile at position 52 does not perturb the His 54−heme loop formation equilibrium under denaturing conditions (3 M gdnHCl), indicating that the conformational properties of the denatured state of iso-1-cytochrome *c* are not affected by the N52I mutation. Figure 3A shows the fluorescence intensity of Trp 59 of AcH54I52 and also of *N*-acetyltryptophanamide (NATA) as a function of pH. NATA is used as a model for the unquenched fluorescence of Trp 59 because the indole ring of NATA is surrounded by two peptide bonds, as is the side chain of Trp 59. The pH profile of the fluorescence intensity of AcH54I52 is very similar to that of the AcH54 variant, and the fluorescence intensity of NATA is essentially invariant with pH. For AcH54I52, the fluorescence drops in the pH range 4−6, is essentially constant in the pH range 6−8, and then rises again at higher pH. Fitting the two transitions to the Henderson−Hasselbalch equation yields pK_a(obs) values of 4.96 ± 0.06 for the low pH transition and 8.69 ± 0.05 for the high pH transition. Both transitions are consistent with one proton processes. The pK_a(obs) for the low pH transition (H_2O to His 54 heme binding) is within error of the pK_a(obs) monitored using the heme Soret band (pK_a(obs) = 4.89 ± 0.03, ref *37*), consistent with the heme Soret band and Trp 59 fluorescence monitoring the same process (His 54 binding to heme) in this pH regime. The high pH process, which must involve displacement of the His 54 ligand, occurs ~1 pH unit higher than the heme Soret monitored binding of a strong field ligand to the AcTM variant (pK_a(obs) ~7.5) where no competing histidines are present. Clearly, the high affinity interaction of His 54 with the heme is able to inhibit the onset of binding of other heme ligands so that, at least in this case, histidine remains the predominate heme ligand in the denatured state up to pH 8. Analysis of the high pH transition for AcH54 (Figure 2C) with the Henderson−Hasselbalch equation gives a pK_a(obs) of 9.0 ± 0.1. Thus, the heme ligation behavior of the AcH54 and AcH54I52 proteins in the high pH regime is similar.

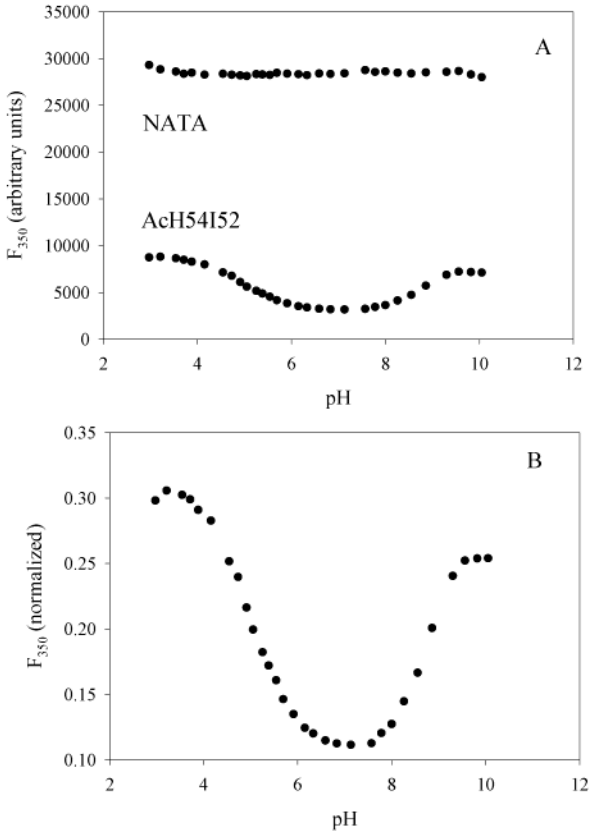

FIGURE 3: pH dependence of the Trp 59 fluorescence of the AcH54I52 variant relative to the fluorescence of NATA (unquenched donor) in the denatured state (3 M gdnHCl). (A) The fluorescence at 350 nm, F_{350}, of Trp 59 in AcH54I52 and of NATA after subtraction of a blank sample at each pH. (B) The fluorescence intensity of the protein normalized to that of NATA, F_{350}(normalized), calculated as the ratio of the fluorescence of protein to that of NATA at each pH value. The fluorescence of the blank, the NATA sample, and the protein sample were measured simultaneously at each pH value. The concentration of both the NATA and the protein was 3 μM. Excitation was at 287 nm, and emission was monitored at 350 nm. Measurements were made at room temperature, 22 ± 1 °C.

The Trp 59−heme emission data in Figure 3 can be used to estimate average heme−Trp 59 separation. The average distance, *R*, for a donor−acceptor pair is given by eq 3 (*32*), where *E* is the efficiency of energy transfer, and $E = 1 - F_{350}$(normalized), where F_{350}(normalized) is the ratio of the Trp 59 emission intensity of denatured cytochrome *c* to that of NATA (emission in the absence of an acceptor), as shown in Figure 3B for AcH54I52.

$$R = R_o((1 - E)/E)^{1/6} \quad (3)$$

The Förster characteristic distance, R_o, is ~30 Å for the Trp−heme donor−acceptor pair (*26*, *33*). Using eq 3, we obtain an average heme−Trp 59 separation of 26.4 ± 0.2 Å (range of two experiments) at low pH (water bound to the sixth coordination site). When His 54 is bound, the average heme−Trp 59 separation is 20.7 ± 0.5 Å (range of two experiments). At high pH, after His 54 is titrated off the heme, the average heme−Trp 59 separation is 25.1 ± 0.1 Å (range of two experiments).

Denatured State Loop Formation with Single Histidine Variants. In previous work (*19*, *20*), we have assembled a large data set of denatured state loop formation affinities,

Table 1: Parameters from Denatured State Titrations of Histidine−Heme Ligation for AcHX Variants as a Function of Protein Concentration in 3 M GdnHCl at 22 °C

variant	[protein] (μM)	pK_a(obs)	*n*
AcH22	1	5.46 ± 0.03	1.00 ± 0.07
	3	5.12 ± 0.10	1.21 ± 0.15
	7.5	4.92 ± 0.04	1.13 ± 0.04
	15	4.81 ± 0.06	1.18 ± 0.07
	30	4.63 ± 0.03	1.06 ± 0.20
	60	4.40 ± 0.08	1.05 ± 0.15
AcH27	1	5.72 ± 0.04	1.25 ± 0.13
	3	5.68 ± 0.03	1.09 ± 0.07
	7.5	5.59 ± 0.03	1.04 ± 0.04
	15	5.61 ± 0.04	1.04 ± 0.12

pK_a(obs), for histidine−heme ligation under denaturing conditions (3 M gdnHCl). To provide additional data for thermodynamic analysis of lysine−heme ligand binding (see Discussion), we have prepared one additional single histidine variant, AcH22. Single histidine variants of iso-1-cytochrome *c* are relatively easily prepared as compared to single lysine variants (15 lysines in the wild-type protein). Thus, the loop size dependence of denatured state heme−ligand equilibria, pK_a(obs), can be more readily obtained for single histidine variants (AcHX). This loop size dependence can then be used in analyzing the competition for heme binding among the 15 lysines in the denatured state of iso-1-cytochrome *c*.

Since formation of short denatured state histidine−heme loops has demonstrated some dependence on protein concentration (AcH11, loop size = 4, ref *20*), we provide a broad concentration dependence for histidine−heme loop formation for the AcH22 variant (loop size = 5). We also provide the concentration dependence for histidine−heme loop formation for the previously reported AcH27 variant (loop size = 10) as a means of assessing the loop size at which intermolecular contributions to loop formation are no longer important for C-terminal loop formation.

In Table 1, the pK_a(obs) and *n* parameters for the AcH22 and AcH27 variants as a function of concentration are shown. As expected, *n*, the number of protons involved in the process is near 1 (see Figure 1). For the AcH22 variant, there is clear concentration dependence for the pK_a(obs) for histidine−heme ligation in 3 M gdnHCl. Within error, there is no significant concentration dependence of the pK_a(obs) for the AcH27 variant. GdnHCl denaturation data, presented in Table 2, demonstrate that both proteins are fully unfolded under the conditions used to measure denatured state loop formation. Quantitative analysis of the pK_a(obs) data to extract intermolecular, K_{inter}, and intramolecular, K_{intra} (heme−ligand binding affinity extrapolated to 0 M protein concentration), histidine−heme binding constants show that intermolecular heme binding is significant for His 22 and insignificant for His 27 binding (Table 3). At 3 μM protein concentration (our standard conditions) in 3 M gdnHCl, His 22−heme binding is ~75% intramolecular, whereas His 27−heme binding is essentially completely intramolecular (Table 3).

In previous work (*20*), intermolecular binding was observed for the short 4 residue loop required by His 11−heme binding but not for the 11 and 16 residue loops formed by His 4 and His(-2)−heme binding. In agreement with this result, we find an intermolecular component for the short 5 residue loop formed by His 22 but not for the 10 residue loop formed by His 27. As previously suggested for AcH11 (*20*), the small size of the intramolecular loop and the close approach of the two hemes in intermolecular binding likely enhance intermolecular His−heme binding relative to intramolecular His−heme loop formation in the denatured state of AcH22.

Table 2: Thermodynamic Parameters from gdnHCl Denaturation of Iso-1-cytochrome *c* Variants at pH 7 and 25 °C

protein	$\Delta G_u(H_2O)$ (kJ/mol)	*m*-value (kJ/mol M)	C_m (M)
WT (C102S)[a]	24.1 ± 1.7	21.4 ± 1.5	1.13 ± 0.02
AcTM[b]	16.4 ± 0.6	15.5 ± 0.8	1.06 ± 0.01
Histidine variants			
AcH22	13.7 ± 0.6	21.4 ± 1.0	0.64 ± 0.01
AcH27[b]	11.5 ± 0.3	18.2 ± 0.7	0.63 ± 0.01
Glutamine variants			
AcQ4Q5	13.4 ± 0.5	12.8 ± 1.2	1.05 ± 0.07
AcQ11	14.1 ± 1.1	22.3 ± 0.8	0.64 ± 0.01
AcQ22	12.4 ± 0.5	13.4 ± 0.3	0.94 ± 0.02
AcQ27	16.9 ± 0.6	15.5 ± 0.6	1.09 ± 0.03
AcQ54Q55	12.7 ± 0.3	12.8 ± 0.3	0.99 ± 0.01

[a] Taken from ref *18*. [b] Taken from ref *19*.

Table 3: Intramolecular and Intermolecular Components of Heme−Ligand Equilibria in 3 M gdnHCl at 22 °C

variant	K_{intra}	K_{inter}	% intramolecular at 3 μM[a]
AcTM	$2.7 \pm 0.5 \times 10^{-8}$ (7.57 ± 0.17)[c]	0 ± 0.0009[b]	103 ± 6
Histidine variants			
AcH22	$5.8 \pm 1.0 \times 10^{-6}$ (5.24 ± 0.18)[c]	1.17 ± 0.07	77 ± 3
AcH27	$2.1 \pm 0.2 \times 10^{-6}$ (5.67 ± 0.07)[c]	0.06 ± 0.04	96 ± 2
Glutamine variants			
AcQ4Q5[d]	5.1×10^{-9} (8.29)[c]	0.0013	72
AcQ11	$2.5 \pm 0.3 \times 10^{-8}$ (7.60 ± 0.13)[c]	0.0012 ± 0.0004	93 ± 2
AcQ22	$2.2 \pm 0.1 \times 10^{-8}$ (7.66 ± 0.03)[c]	0.0006 ± 0.0001	96 ± 1
AcQ27	$2.8 \pm 0.5 \times 10^{-8}$ (7.56 ± 0.18)[c]	0.0013 ± 0.0010	93 ± 5
AcQ54Q55[d]	2.1×10^{-8} (7.69)[c]	0.0002	98

[a] % intramolecular at 3 μM = $\{K_{intra}/(K_{intra} + K_{inter} \times 3 \times 10^{-6}\ M)\} \times 100$. Error obtained by standard propagation of the error in K_{inter} and K_{intra}. [b] The slope of eq 2 was negative giving $K_{inter} = -2.4 \times 10^{-4}$, a physically undefined value. This value, however, was used to calculate the magnitude and the error for % intramolecular. [c] The number in brackets given below each K_{intra} value is the pK_a(obs) at zero protein concentration, calculated as $-\log(K_{intra})$. [d] pK_a(obs) was only obtained at two protein concentrations, so the error in K_{intra} and K_{inter} from the fit to eq 2 is indeterminate.

Effect of Removal of Lysine Side Chains on Denatured State Loop Formation in the Absence of Histidine. The fluorescence data in Figure 2 indicate that lysines 54/55 are not the primary heme ligands in the denatured state (3 M gdnHCl) of iso-1-cytochrome *c*. The lack of increased Trp 59 quenching by heme above pH 7 for AcTM and AcH26 and the decrease in Trp 59 quenching by heme indicate that the high pH heme ligand in the denatured state is either near the heme or on the N-terminal side of the site of heme attachment. Our recent results on N-terminal AcHX variants (*20*) support the latter possibility and indicate that lysines

Table 4: Parameters from Denatured State Titrations of Histidine−Heme Ligation for AcQX Variants as a Function of Protein Concentration in 3 M gdnHCl at 22 °C

variant	[protein] (μM)	pK_a(obs)	n
AcTM	3	7.62 ± 0.05	1.02 ± 0.05
	7.5	7.55 ± 0.04	0.94 ± 0.05
	15	7.66 ± 0.03	0.90 ± 0.09
AcQ4Q5	3	8.15 ± 0.03	0.92 ± 0.07
	7.5	8.00 ± 0.05	0.87 ± 0.09
AcQ11	3	7.61 ± 0.04	0.86 ± 0.06
	7.5	7.49 ± 0.02	0.8 ± 0.06
	30	7.37 ± 0.02	1.02 ± 0.09
AcQ22	3	7.65 ± 0.08	0.99 ± 0.08
	7.5	7.61 ± 0.03	0.94 ± 0.02
	15	7.58 ± 0.06	0.81 ± 0.05
AcQ27	3	7.56 ± 0.05	0.94 ± 0.09
	7.5	7.44 ± 0.03	0.99 ± 0.04
	15	7.44 ± 0.02	0.77 ± 0.04
AcQ54Q55	3	7.68 ± 0.12	0.83 ± 0.04
	7.5	7.67 ± 0.07	0.88 ± 0.03

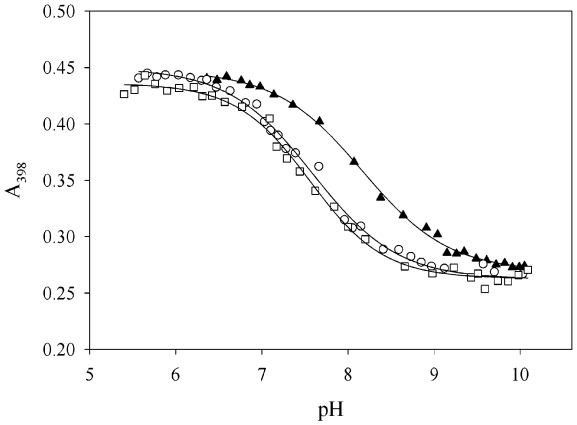

FIGURE 4: Denatured state heme−ligand titrations for lysine → glutamine variants of iso-1-cytochrome *c*. Titrations for AcQ11 (open circles), AcQ27 (open squares), and AcQ4Q5 (solid triangles) were carried out at 3 μM protein concentration, in 3 M gdnHCl, 5 mM Na_2HPO_4, and 15 mM NaCl at 22 ± 1 °C. Solid curves are fits of the data to eq 1 in the Materials and Methods. Parameters from the fits of eq 1 to the data are collected in Table 4.

4/5 are the most likely ligands. However, other amino acids side chains, such as tyrosine, are known to act as heme ligands in proteins (*47*, *48*). Thus, to definitively ascertain the primary heme ligand above pH 7 under denaturing conditions, we have individually replaced lysines near the heme at positions 11, 22, and 27 with glutamine (AcQ11, AcQ22, and AcQ27). Lysines 4/5 and 54/55 have been replaced with glutamine simultaneously (AcQ4Q5 and AcQ54Q55).

If there is a predominate lysine ligand, then when this lysine is replaced with glutamine there should be a significant shift upward in the pK_a(obs) for heme−ligand ligation relative to the AcTM variant. In Table 2, gdnHCl denaturation data demonstrate that all variants are completely unfolded under the conditions (3 M gdnHCl) used to measure denatured state loop equilibria. In Table 4, the pK_a(obs) data for these variants, as well as for the AcTM variant, are shown as a function of protein concentration. All heme ligand titrations are approximately 1 proton processes (Table 4), as expected (see Figure 1). The concentration dependence of pK_a(obs) is also minimal such that, for the most part, the observed titration is essentially completely intramolecular at 3 μM protein concentration (Table 3). Similarly, comparison of pK_a(obs) at 0 M protein concentration (bracketed values in Table 3) with pK_a(obs) at 3 μM protein concentration shows that these two quantities are generally within error of each other. For the AcQ11, AcQ22, AcQ27, and AcQ54Q55 variants, pK_a(obs) does not change significantly relative to AcTM, indicating that none of these lysines is the predominate heme ligand under denaturing conditions above pH 7. On the other hand, there is a significant upward shift in the pK_a(obs), of ∼0.5 units, for the AcQ4Q5 variant relative to the AcTM and other AcQX variants (Figure 4). This result clearly implicates lysines 4 and 5 as the primary heme ligands in the titration observed near pH 7.6 for the AcTM variant.

DISCUSSION

Heme Ligands as a Function of pH in Denatured Iso-1-cytochrome c. In previous work on heme ligation, the emphasis has been on observing changes in heme ligation from neutral to acidic pH. In general, the topological constraints on the denatured state of cytochrome *c* imposed by heme ligation have been attributed to histidine−heme loop formation (*21*−*25*). However, work from this laboratory has demonstrated that in the absence of histidine (and with a blocked N-terminal amino group), another strong field ligand is capable of binding to the heme of denatured iso-1-cytochrome *c* with a pK_a(obs) of ∼7.5 (*19*, *27*). Since denatured state heme ligation strongly affects the energy landscape and thus the mechanism for folding cytochrome *c* (*23*−*27*), knowledge of the changes in heme ligation in the denatured state as a function of solution pH is important.

The ϵ-amino group of lysine is known to have a high affinity for heme binding (*28*, *45*) and thus is a likely candidate. However, tyrosinate has been implicated as a ligand capable of leading to low spin Tyr^-/His ligation of ferric heme in both proteins (*47*) and heme−peptides (*48*), and iso-1-cytochrome *c* has tyrosines at positions 46, 48, 67, and 74. Since each of these tyrosines would bring Trp 59 within 15 residues of the heme, it seems likely that some additional quenching of Trp 59 fluorescence would have been observed for the AcH26 and AcTM variants at high pH, in the denatured state, if these tyrosine residues were involved in heme binding. Our work on histidine−heme loop formation in denatured iso-1-cytochrome *c* (3 M gdnHCl) suggested that lysines 4 and 5 would be strong candidates for the high pH ligands (*20*). This prediction is consistent with the observation that no decrease in fluorescence intensity occurs at high pH in 3 M gdnHCl for the AcTM and AcH26 variants and that the loss of His 54 binding in the AcH54 and AcH54I52 variants leads to an increase in Trp 59 fluorescence intensity at high pH. When lysines in the AcTM variant of iso-1-cytochrome *c* are replaced with glutamine, no effect on the denatured state pK_a(obs) occurs for lysines at positions 11, 22, 27, 54, or 55 (AcQ11, AcQ22, AcQ27, and AcQ54Q55) relative to the AcTM variant. However, replacement of lysines 4 and 5 with glutamine (AcQ4Q5) leads to a 0.5 unit upward shift in the pK_a(obs) of the AcTM variant. This observation clearly implicates lysines 4 and 5 as the predominate ligands for the sixth coordination site of

the heme in the denatured state of cytochrome *c*, above neutral pH. The data also allow us to definitively rule out the participation of tyrosines 46, 48, 67, and 74 in heme ligation in the denatured state of cytochrome *c* in this pH regime.

Competition between Histidine and Lysine Ligation Near Neutral pH. For most studies on the folding mechanism of cytochrome *c*, histidine residues are present. Thus, it is important to understand how histidine and lysine compete for heme ligation in the denatured state. At what pH does lysine ligation start to contribute to the constraints on the denatured state of cytochrome *c* and thus affect the folding of this protein?

The data on AcH54 and AcH54I52 in Figures 2C and 3 allow analysis of the competition between histidine and lysine ligands for the sixth coordination site of the heme, under denaturing conditions. The loop formation equilibrium for histidine or lysine binding to the heme of denatured cytochrome *c* can be broken down into a stepwise equilibrium involving, first, ionization of the ligand, followed by binding of the neutral ligand to the heme. Eq 4 expresses this stepwise process

$$pK_a(\text{obs}) = pK_a(LH^+) + pK_{FeL} \quad (4)$$

where pK_a(obs) is the experimental midpoint for loop formation in 3 M gdnHCl, $pK_a(LH^+)$ is the acid ionization constant of the protonated form of the ligand, and pK_{FeL} is the affinity of the neutral form of the ligand for the heme of denatured cytochrome *c*. For His 54 in AcH54, if we use $pK_a(HisH^+)$ ~6.5, then pK_{FeL} is approximately −1.6 (pK_a(obs) ~4.9 for AcH54 and AcH54I52; see Results and ref *19*). For AcTM, if we assume lysine ligands with a $pK_a(LysH^+)$ ~10.5, then the effective pK_{FeL} for these lysine ligands is approximately −2.9 (using pK_a(obs) ~7.6 for AcTM, see Table 4). The value of pK_{FeL} is the upper limit for the affinity of the ligand for the heme (i.e., the affinity at pH values significantly above $pK_a(LH^+)$). For AcH54 and AcH54I52, the high pH loss of His 54 binding occurs above pH 8, so we can assume that the affinity of His 54 for the heme has reached its maximal value of pK_{FeL} approximately −1.6 (since $pK_a(HisH^+)$ ~6.5). At the midpoint for loss of His 54 binding at alkaline pH (Figures 2C and 3), the affinity of His 54 (pK_{FeL} approximately −1.6) must equal the effective affinity of the lysine ligands. The affinity of an ionizable ligand for the heme is diminished as the pH drops below $pK_a(LH^+)$ according to eq 5 (*49*), where $K_{FeL}(H^+)$ is the affinity of the ionizable ligand, L, at a given $[H^+]$. For $[H^+] \gg K_a(LH^+)$, the 1 in the denominator can be neglected.

$$K_{FeL}(H^+) = \frac{K_{FeL}}{[1 + \{[H^+]/K_a(LH^+)\}]} \quad (5)$$

Expressing this simplification of eq 5 in p*K* notation, we obtain eq 6.

$$pK_{FeL}(H^+) \approx pK_{FeL} + (pK_a(LH^+) - \text{pH}) \quad (6)$$

Using $pK_{FeL} = -2.9$ and $pK_a(LH^+) = 10.5$, the effective affinity of the lysine ligands for the heme is expected to match the affinity of His 54 ($pK_{FeL}(H^+) = -1.6$) in AcH54 or AcH54I52 at ~pH 9.2. Given the approximations in this calculation, this value matches reasonably well the observed pH range of 8.7−9.0 for the midpoint of the loss of His 54−heme binding in these two proteins.

Knowing the midpoint for loss of His 54 binding at high pH from our data in Figures 2C and 3, we can predict the midpoint for the transition from histidine to lysine ligation, $pH_{His/Lys}$(Variant), in other proteins (such as AcH26) even though direct observation of this change in ligation was not possible in Figure 2B. It can be shown, from consideration of eqs 4 and 6 and the requirement that $pK_{FeL}(H^+)$ for lysine−heme ligation and pK_{FeL} for histidine−heme ligation must be the same at $pH_{His/Lys}$(Variant) for denatured iso-1-cytochrome *c*, that eq 7 can be used to predict $pH_{His/Lys}$ (Variant). In this equation, the pK_a(obs) values are the experimentally measured values for histidine−heme loop formation under denaturing conditions (3 M gdnHCl).

$$pH_{His/Lys}(\text{Variant}) = pH_{His/Lys}(\text{His 54}) - (pK_a(\text{obs})_{\text{Variant}} - pK_a(\text{obs})_{\text{His54}}) \quad (7)$$

Thus, for the AcH26 variant, $pH_{His/Lys}$(AcH26) is predicted to be ~8.4, using $pH_{His/Lys}$(His 54) ~8.8, $pK_a(\text{obs})_{\text{His54}} = 4.9$, and $pK_a(\text{obs})_{\text{His26}} = 5.3$ (*19*). For WT iso-1-cytochrome *c*, where His 26, 33, and 39 compete for ligation to the heme under denaturing conditions, pK_a(obs) is ~4.7 (*34*). Therefore, the midpoint for the transition from histidine to lysine ligation, $pH_{His/Lys}$(WT), is expected to be ~9.0 (with an acetylated N-terminus). Thus, for WT iso-1-cytochrome *c* and many of the single histidine variants (AcHX) that we have studied, histidine is expected to be the primary heme ligand below pH 8.0. For lysines to bind to the heme and affect the topology of the denatured state of this protein, the pH must be significantly above physiological values. However, when this His → Lys ligation change occurs, the topology of the denatured state will change dramatically from one involving a C-terminal loop (His 26, 33, or 39 in the WT protein) to one involving an N-terminal loop (Lys 4 and 5), strongly altering the starting point for folding.

Quantitative Assessment of the Contribution of Individual Lysines to Heme Ligation Under Denaturing Conditions Above Neutral pH. There are lysines at positions −2, 4, 5, 11, 22, 27, 54, 55, 73, 79, 86, 87, 89, 99, and 100 in iso-1-cytochrome *c*. With so many ligands competing for heme ligation in the denatured state at higher pH, there is expected to be some heterogeneity in the constraints on the denatured state of cytochrome *c* under these conditions. Heterogeneity in the denatured state could impact the folding mechanism of this protein. To directly assess the individual affinities of each lysine for the heme of denatured cytochrome *c* would require a large and probably infeasible amount of mutagenesis. However, a simple thermodynamic analysis using denatured state histidine−heme binding data (Table 5) can provide this information.

Consideration of the expression for pK_a(obs) in eq 4 for heme−ligand affinity is key to this analysis. First, we assume that the pK_a of an ionizable amino acid side chain, $pK_a(LH^+)$, is insensitive to sequence position in concentrated gdnHCl solution. This assumption is reasonable based on the work of Tanford and Nozaki (*50*). Thus, the variation in pK_a(obs) is due primarily to pK_{FeL}, which depends on sequence position (loop size and topology, see refs *17*−*20*). This sequence position effect should be the same irrespective of

Table 5: Compilation of pK_a(obs) and K_{FeL} Values for AcHX Variants of Iso-1-cytochrome *c* at 3 μM Protein Concentration and 22 °C at Lysine Sequence Positions

variant	pK_a(obs)	K_{FeL}[a]
AcH4	4.22 ± 0.03[b]	190.5
AcH11	5.15 ± 0.03[b]	22.4
AcH22	5.12 ± 0.10	24.0
AcH27	5.68 ± 0.03[c]	6.6
AcH54	4.81 ± 0.06[c]	49.0
AcH73	5.63 ± 0.11[c]	7.4
AcH89	5.97 ± 0.06[c]	4.4
AcH100	6.34 ± 0.02[c]	1.4

[a] $K_{FeL} = 10^{-(pK_a(obs)-6.5)}$, where a value of 6.5 is taken for pK_a(HisH$^+$); see eq 4 in the text. [b] Taken from ref *20*. [c] Taken from ref *19*.

the nature of the ligand. Therefore, we can use our database of individual histidine−heme affinities to predict the relative affinities of the 14 lysines in the AcTM variant (in AcTM, Lys(-2) is replaced with Leu). The pK_a(obs) values and the K_{FeL} values (see eq 4) for all AcHX variants are compiled in Table 5. Using these data, we can calculate the expected fractional population of Lys 4/5 ligation under denaturing conditions, $P_{Lys4/5}$, relative to all the other lysines in the AcTM variant of iso-1-cytochrome *c*, using a simple partition function analysis (eq 8).

$$P_{Lys4/5} = [2K_{FeL}(AcH4)]/[\{1 + 2K_{FeL}(AcH4) + K_{FeL}(AcH11) + K_{FeL}(AcH22) + K_{FeL}(AcH27) + 2K_{FeL}(AcH54) + 2K_{FeL}(AcH73) + 3K_{FeL}(AcH89) + 2K_{FeL}(AcH100)\}] \quad (8)$$

Since we have not measured the pK_a(obs) for denatured state loop formation for histidines at all sequence positions corresponding to lysines, it is assumed that K_{FeL} values for positions close in sequence are approximately the same (i.e., K_{FeL}(His 86) + K_{FeL}(His 87) + K_{FeL}(His 89) ≈ 3 × K_{FeL}(AcH89)) since the loops closed upon ligation will be similar in size. Eq 8 predicts $P_{Lys4/5} \approx 0.68$ or 68%. On the other hand, $P_{Lys54/55}$ obtained via an analogous calculation equals 0.17 or 17%. Similar calculations for the other lysines show that Lys 11 and Lys 22 together account for ∼8% of denatured state heme ligation, and the remaining 7 lysines together account for ∼7% of denatured state heme ligation at alkaline pH.

The shift in the pK_a(obs) for AcQ4Q5 relative to AcTM should be related to the change in the magnitude of the partition function for heme−ligand binding, *Z* (denominator in eq 8), when Lys 4/5 are removed from the protein. For AcTM, $Z = 560.9$ while for AcQ4Q5, $Z = 179.8$. The change in the pK_{FeL} (eq 4) for AcTM versus AcQ4Q5 should go as −log *Z*(AcQ4Q5) − (−log *Z*(AcTM) = 0.49. With pK_{FeL} becoming 0.49 units less negative in eq 4, the pK_a(obs) should shift upward by 0.49 units. This is very close to the observed upward shift of 0.53 ± 0.08 units at 3 μM protein concentration (see Table 4). The close correspondence of the experimental and calculated shifts in pK_a(obs) for AcTM versus AcQ4Q5 indicate that the assumptions in eq 8 are reasonable.

We note that the pK_a(obs) for AcQ4Q5 appears to show some concentration dependence (Tables 3 and 4). Use of partition function analysis, as in eq 8, shows that lysines 11 and 22 will contribute ∼26% to the observed denatured state loop equilibrium at 3 μM protein concentration for AcQ4Q5. Both AcH11 and AcH22 have concentration dependent pK_a(obs) values consistent with AcQ4Q5 showing concentration dependence for its pK_a(obs).

Dimension of the Denatured State of Iso-1-cytochrome c as a Function of pH. By analyzing the fluorescence intensity of Trp 59 in AcH54I52 cytochrome *c* relative to NATA (unquenched donor), it is possible to estimate the average heme−Trp 59 distance in denatured cytochrome *c* in 3 M gdnHCl. We find that, at both low and high pH, the heme−Trp 59 distances are similar, ∼26.4 and ∼25.1 Å, respectively. The slight decrease in distance at high pH relative to low pH could reflect some contribution from lysine 55 binding at high pH, in addition to the binding by lysine side chains on the N-terminal side of the heme, as discussed above. Therefore, we will use the low pH distance as a reference point for comparison with the random coil predictions of average heme−Trp 59 distance for a disordered chain running from His 18 to Trp 59 (42 residues). Flory's treatment of disordered polypeptide chains (*9*, *35*, *36*) predicts that the average end-to-end chain separation, $R_{random\ coil}$, is given by eq 9

$$R^2_{random\ coil} = C_n l^2 n \quad (9)$$

where C_n is the characteristic ratio, a measure of chain stiffness, *n* is the number of monomers in the polypeptide, and *l* is the effective bond length of a polypeptide monomer ($l = 3.8$ Å). The characteristic ratio, C_n, is expected to be most sensitive to glycine content, having a value of ∼9 for polyalanine and ∼2 for polyglycine (*35*, *36*). For the sequence between His 18 and Trp 59, the glycine content is ∼20%. The value for C_n is ∼5.2 for 20% glycine content (*51*), giving $R_{random\ coil} = (75n)^{1/2} = 56$ Å for a chain of 42 monomers. Our measured separation is about half this distance, indicating substantial deviation from random coil behavior under our denaturing conditions. This deviation from random coil expectations is consistent with our previous results on the chain length dependence of the pK_a(obs) for denatured state loop formation in 3 M gdnHCl, which also showed strong deviation from random coil behavior (*19*). One possible explanation for the substantially shorter Trp 59−heme distance observed relative to random coil predictions relates to the [gdnHCl] used in these experiments. Previous studies show that 6 M gdnHCl is a Θ solvent (polymer−polymer interactions and excluded volume are exactly counterbalanced) and thus is the [gdnHCl] where random coil behavior is expected (*7*, *9*). At lower concentrations of gdnHCl, the interactions between the monomers in the polypeptide are expected to dominate over excluded volume effects leading to a more compact state (*7*, *9*). Also, these are equilibrium measurements. Recent kinetic fluorescence energy transfer studies on dansylated (at Cys 102) iso-1-cytochrome *c* show that even in 3 M gdnHCl a portion of the protein exists in a compact state (*52*). This compact/extended equilibrium in the denatured state will skew the average distance, *R*, measured by Trp 59/heme quenching to somewhat shorter distances.

When His 54 is bound to the heme in the denatured state, the average Trp 59−heme distance drops to ∼20.7 Å. Given the large decrease in the number of residues separating the

heme and Trp 59 (down to 6 from 42), the small decrease in the heme−Trp 59 distance is surprising. Eq 9 is not straightforward to apply at short chain lengths (i.e., 6 residues) because the magnitude of C_n is not constant and drops dramatically as n approaches zero in eq 9 (*35*, *36*). It is perhaps most useful to compare our measured distance of ~20.7 Å for the His 54−heme ligated state to the expected end-to-end distance for an extended (β conformation) polypeptide chain with $n = 6$, where $R_{extended} = 3.5n = 21$ Å. Our measured value for R is only slightly shorter than the end-to-end distance for an extended polypeptide chain of six residues. Recent results (*53*−*56*) suggest that denatured proteins tend to occupy a polyproline II structure, which is nearly as extended as the β conformation. The tendency to populate the polyproline II structure is enhanced in gdnHCl solutions (*55*, *57*), as used for our measurements. The Trp 59−heme distance we observe for the His 54 bound state in 3 M gdnHCl is consistent with these recent results regarding the population of the polyproline II state in disordered polypeptides (for $n = 6$, $R \sim 3.0n = 18$ Å, see ref *56*). We note, however, that some caution in interpreting the distance in the His 54-bound state should be exercised since the short connecting chain length could limit the freedom of motion of the heme relative to the Trp 59 in the His 54 bound state, even though the protein is denatured. If the orientation factor, κ, were affected, our use of the same value for the Förster characteristic distance for distance calculations in both the His 54 bound and unbound states would be invalid.

CONCLUSION

In these studies, we have probed the pH dependence of the constraints acting upon the denatured state of iso-1-cytochrome *c*. The observed changes in these constraints would be expected to affect the folding mechanism of this protein. A combination of fluorescence and mutagenesis studies demonstrates that lysines 4 and 5 are the predominate heme ligands in the denatured state of this protein at alkaline pH. For most cytochromes *c*, Lys 4/5−heme ligation will significantly change the topology of the denatured state from C-terminal (His−heme ligation) to N-terminal heme−ligand loop constraints as the pH is raised. Partition function analysis of the relative affinity of the lysine ligands in cytochrome *c* based on sequence position indicates that lysines 4 and 5 will account for 68% of denatured state heme ligation at alkaline pH, with other lysines providing 32% of the heme ligation. Thus, substantial heterogeneity will exist in the constraints operating on the denatured state of cytochrome *c* under alkaline conditions. Analysis of the thermodynamics of competition between histidine and the high pH ligands indicates that histidines (and the N-terminal amino group, if not acetylated) will be the primary heme ligands causing misfolding of iso-1-cytochrome *c* for pH values below 8.0. Finally, evaluation of the heme−Trp 59 distance in denatured iso-1-cytochrome *c*, using Förster energy transfer theory, is consistent with the cytochrome *c* denatured state in 3 M gdnHCl being much more compact than expected for a random coil, as observed for many proteins (*7*, *8*, *10*). The heme−Trp 59 distance data for the His 54−heme bound denatured state indicate that for short segments of polypeptide, the polypeptide conformation is predominately extended. This observation is consistent with recent results (*53*−*56*) indicating substantial population of the polyproline II conformation in disordered polypeptides.

REFERENCES

1. Englander, S. W. (2000) Protein folding intermediates and pathways studied by hydrogen exchange, *Annu. Rev. Biophys. Biomol. Struct. 29*, 213−238.
2. Dill, K. A. (1999) Polymer principles and protein folding, *Protein Sci. 8*, 1166−1180.
3. Pain, R. H. (2000) *Mechanisms of Protein Folding*, 2nd ed. (Pain, R. H., Ed.) Oxford University Press, Oxford.
4. Murphy, K. P. (2001) *Protein Structure, Stability, and Folding* (Murphy, K. P., Ed.) Humana Press, Totowa, NJ.
5. Levinthal, C. (1968) Are there pathways for protein folding? *J. Chim. Phys. 65*, 44−45.
6. Dill, K. A., and Chan, H. S. (1997) From Levinthal to pathways to funnels, *Nat. Struct. Biol. 4*, 10−19.
7. Dill, K. A., and Shortle, D. (1991) Denatured states of proteins, *Annu. Rev. Biochem. 60*, 795−825.
8. Shortle, D. (1995) Staphylococcal nuclease: A showcase of *m*-value effects, *Adv. Protein Chem. 46*, 217−247.
9. Tanford, C. (1968) Protein denaturation, *Adv. Protein Chem. 23*, 121−282.
10. Shortle, D. (1996) Structural analysis of non-native states of proteins by NMR methods, *Curr. Opin. Struct. Biol. 6*, 24−30.
11. Dyson, H. J., and Wright, P. E. (1998) Equilibrium NMR studies of unfolded and partially folded proteins, *Nat. Struct. Biol. 5*, 499−503.
12. Zhang, O., and Forman-Kay, J. (1997) NMR studies of unfolded states of an SH3 domain in aqueous solution and denaturing conditions, *Biochemistry 36*, 3959−3970.
13. Mok, Y.-K., Kay, C. M., Kay, L. E., and Forman-Kay, J. (1999) NOE data demonstrating a compact unfolded state for an SH3 domain under nondenaturing conditions, *J. Mol. Biol. 289*, 619−638.
14. Klein-Seetharaman, J., Oikawa, M., Grimshaw, S. B., Wirmer, J., Duchardt, E., Ueda, T., Imoto, T., Smith, L. J., Dobson, C. M., and Schwalbe, H. (2002) Long-range interactions within a nonnative protein, *Science 295*, 1719−1722.
15. Gillespie, J. R., and Shortle, D. (1997) Characterization of long-range structure in the denatured state of staphylococcal nuclease. II. Distance restraints from paramagnetic relaxation and calculation of an ensemble of structures, *J. Mol. Biol. 268*, 170−184.
16. Shortle, D., and Ackerman, M. S. (2001) Persistence of nativelike topology in a denatured protein in 8 M urea, *Science 293*, 487−489.
17. Godbole, S., and Bowler, B. E. (1997) A histidine variant of yeast iso-1-cytochrome *c* that strongly affects the energetics of the denatured state, *J. Mol. Biol. 268*, 816−821.
18. Godbole, S., Hammack, B., and Bowler, B. E. (2000) Measuring denatured state energetics: Deviations from random coil behavior and implications for the folding of iso-1-cytochrome *c*, *J. Mol. Biol. 296*, 217−228.
19. Hammack, B. N., Smith, C. R., and Bowler, B. E. (2001) Denatured state thermodynamics: Residual structure, chain stiffness, and scaling factors, *J. Mol. Biol. 311*, 1091−1104.
20. Smith, C. R., Mateljevic, N., and Bowler, B. E. (2002) Effect of topology and excluded volume on protein denatured state conformational properties, *Biochemistry 41*, 10173−10181.
21. Babul, J., and Stellwagen, E. (1971) The existence of heme-protein coordinate-covalent bonds in denaturant solvents, *Biopolymers 10*, 2359−2361.
22. Muthukrishnan, K., and Nall, B. T. (1991) Effective concentrations of amino acid side chains in an unfolded protein, *Biochemistry 30*, 4706−4710.
23. Elöve, G. A., Bhuyan, A. B., and Roder, H. (1994) Kinetic mechanism of cytochrome *c* folding: Involvement of the heme and its ligands, *Biochemistry 33*, 6925−6935.
24. Colón, W., Wakem, L. P., Sherman, F., and Roder, H. (1997) Identification of the predominant non-native histidine ligand in unfolded cytochrome *c*, *Biochemistry 36*, 12535−12541.
25. Sosnick, T. R., Mayne, L., and Englander S. W. (1994) The barriers in protein folding, *Nat. Struct. Biol. 1*, 149−156.
26. Pierce, M. M., and Nall, B. T. (1997) Fast folding of cytochrome *c*, *Protein Sci. 6*, 618−627.
27. Hammack, B., Godbole, S., and Bowler, B. E. (1998) Cytochrome *c* folding traps are not due solely to histidine-heme ligation: Direct

demonstration of a role for N-terminal amino group-heme ligation, *J. Mol. Biol. 275*, 719−724.
28. Russel, B. S., Melenkivitz, R., and Bren, K. L. (2000) NMR investigation of ferricytochrome *c* unfolding: Detection of an equilibrium unfolding intermediate and residual structure in the denatured state, *Proc. Natl. Acad. Sci. U.S.A.* 97, 8312−8317.
29. Tsong, T. Y. (1974) The Trp-59 fluorescence of ferricytochrome *c* as a sensitive measure of the overall protein conformation, *J. Biol. Chem. 249*, 1988−1990.
30. Brayer, G. D., and Murphy, M. E. P. (1996) Structural studies of eukaryotic cytochromes *c*, in *Cytochrome c: A Multidisciplinary Approach*, (Scott, R. A., and Mauk, A. G., Eds.) pp 103−166, University Science Books, Sausilito, CA.
31. Tsong, T. Y. (1976) Ferricytochrome *c* chain folding measured by the energy transfer of tryptophan 59 to the heme group, *Biochemistry 15*, 5467−5473.
32. Stryer, L. (1978) Fluorescence energy transfer as a spectroscopic ruler, *Annu. Rev. Biochem. 47*, 819−846.
33. Stryer, L. (1959) Intramolecular resonance energy transfer in proteins, *Biochim. Biophys. Acta 35*, 242−244.
34. Godbole, S., Dong, A., Garbin, K., and Bowler, B. E. (1997) A lysine 73 → histidine variant of yeast iso-1-cytochrome *c*: Evidence for a nativelike intermediate in the unfolding pathway and implications for *m*-value effects, *Biochemistry 36*, 119−126.
35. Flory, P. J. (1969) *Statistical Mechanics of Chain Molecules*, pp 248−306, John Wiley & Sons, New York.
36. Cantor, C. R., and Schimmel, P. R. (1980) *Biophysical Chemistry, Part III: The Behavior of Biological Macromolecules*, pp 979−1018, W. H. Freeman and Co., San Francisco, CA.
37. Hammack, B. N. Effects of yeast iso-1-cytochrome *c* histidine variants on denatured state energetics, Ph.D. Dissertation, University of Denver, Denver, CO, 2000.
38. Das, G., Hickey, D. R., McLendon, D., McLendon, G., and Sherman, F. (1989) Dramatic thermostabilization of yeast iso-1-cytochrome *c* by an asparagine → isoleucine replacement at position 57, *Proc. Natl. Acad. Sci. U.S.A. 86*, 496−499.
39. Deng, W. P. D., and Nickoloff, J. A. (1992) Site-directed mutagenesis of virtually any plasmid by eliminating a unique site, *Anal. Biochem. 200*, 81−88.
40. Bowler, B. E., May, K., Zaragoza, T., York, P., Dong, A., and Caughey, W. S. (1993) Destabilizing effects of replacing a surface lysine of cytochrome *c* with aromatic amino acids: Implications for the denatured state, *Biochemistry 32*, 183−190.
41. Pace, C. N. (1986) Determination and analysis of urea and guanidine hydrochloride denaturation curves, *Methods Enzymol. 113*, 266−280.
42. Gill, S. C., and von Hippel, P. H. (1989) Calculation of protein extinction coefficients from amino acid sequence data, *Anal. Biochem. 182*, 319−326.
43. Herrmann, L., Bowler, B. E., Dong, A., and Caughey, W. S. (1995) The effects of hydrophilic to hydrophobic surface mutations on the denatured state of iso-1-cytochrome *c*: Investigation of aliphatic residues, *Biochemistry 34*, 3040−3047.
44. Schellman, J. A. (1978) Solvent denaturation, *Biopolymers 17*, 1305−1322.
45. Pollock, W. B. R., Rosell, F. I., Twitchett, M. B., Dumont, M. E., and Mauk, A. G. (1998) Bacterial expression of a mitochondrial cytochrome *c*. Trimethylation of Lys72 in yeast iso-1-cytochrome *c* and the alkaline conformational transition, *Biochemistry 37*, 6124−6131.
46. Pierce, M. M., and Nall, B. T. (2000) Coupled kinetic traps in cytochrome *c* folding: His-heme misligation and proline isomerization, *J. Mol. Biol. 298*, 955−969.
47. Das, T. K., Couture, M., Lee, H. C., Peisach, J., Rousseau, D. L., Wittenberg, B. A., Wittenberg, J. B., and Guertin, M. (1999) Identification of the ligands to the ferric heme of *Chlamydomonas* chloroplast hemoglobin: Evidence for ligation of tyrosine-63 (B10) to the heme, *Biochemistry 38*, 15360−15368.
48. Low, D. W., Yang, G., Winkler, J. R., and Gray, H. B. (1999) Modification of heme peptides by reverse proteolysis: Spectroscopy of microperoxidase-10 with C-terminal histidine, tyrosine, and methionine residues, *J. Am. Chem. Soc. 119*, 4094−4095.
49. Adams, P. A., Baldwin, D. A., and Marques, H. M. (1996) The hemepeptides from cytochrome *c*: Preparation, physical and chemical properties, and their use as model compounds for the hemoproteins, in *Cytochrome c: A Multidisciplinary Approach* (Scott, R. A., and Mauk, A. G., Eds.) pp 635−694, University Science Books, Sausalito, CA.
50. Nozaki, Y., and Tanford, C. (1967) Protein random coils. II. Hydrogen ion titration curve of Ribonuclease in 6 M guanidine hydrochloride, *Biochemistry 89*, 742−749.
51. Miller, W. G., Brant, D. A., and Flory, P. J. (1967) Random coil configurations of polypeptide copolymers, *J. Mol. Biol. 23*, 67−80.
52. Lyubovitsky, J. G., Gray, H. B., and Winkler, J. R. (2002) Mapping the cytochrome *c* folding landscape, *J. Am. Chem. Soc. 124*, 5481−5485.
53. Shi, Z., Olson, C. A., Rose, G. D., Baldwin, R. L., and Kallenbach, N. R. (2002) Polyproline II structure in a sequence of seven alanine residues, *Proc. Natl. Acad. Sci. U.S.A. 99*, 9190−9195.
54. Rucker, A. L., and Creamer, T. P. (2002) Polyproline II helical structure in protein unfolded states: Lysine peptides revisited, *Protein Sci. 11*, 980−985.
55. Kelly, M. A., Chellgren, B. W., Rucker, A. L., Troutman, J. M., Fried, M. G., Miller, A. F., and Creamer, T. P. (2001) Host−guest study of left-handed polyproline II helix formation, *Biochemistry 40*, 14376−14383.
56. Pappu, R. V., and Rose, G. D. (2002) A simple model for polyproline II structure in unfolded states of alanine-based peptides, *Protein Sci. 11*, 2437−2455.
57. Woody, R. W. (1992) Circular dichroism and conformation of unordered polypeptides, *Adv. Biophys. Chem. 2*, 15376−14383.

BI026827I